LAWRENCE
LIVERMORE
NATIONAL
LABORATORY

LLNL-TR-568072

Evaluating Use of Satellite Observations for Detecting Large CO2 Leaks and Carbon Sequestration Monitoring

W. Brewer, G. Hoffman, E. Silver, C. DiLeonardo, J. R. Henderson, S. Vigil

August 1, 2012

Disclaimer

This work performed under the auspices of the U.S. Department of Energy by Lawrence Livermore National Laboratory under Contract DE-AC52-07NA27344.

Evaluating Use of Satellite Observations for Detecting Large CO_2 Leaks and Carbon Sequestration Monitoring

William Brewer, Gary Hoffmann, Eli Silver

Earth and Planetary Sciences Department, University of California, Santa Cruz, CA

Christopher DiLeonardo

De Anza College, Cupertino, CA

John Henderson

Lawrence Livermore National Security, Livermore, CA

Sam Vigil

California Polytechnic State University, San Luis Obispo, CA

November 3rd , 2011

Abstract

We tested the feasibility of orbital CO_2 sensors as detectors of leaks from sequestration sites using the SCIAMACHY and GOSAT instruments. From the footprint size of each instrument we calculated the atmospheric volume sampled by SCIAMACHY and GOSAT readings, and from this data the amount of CO_2 leakage necessary to measurably impact readings from the instruments. We used a high-emission coal electric plant as a baseline leak quantity, which is a substantially larger amount of CO_2 than would be expected from a sequestration leak. Nonetheless, the plant's output is not detectable by either instrument. Geospatial and geostatistical analysis of collected data supports this conclusion. SCIAMACHY data from the summer of 2005 over the contiguous US showed broad topographic patterns in CO_2 distribution, with the eastern flanks of mountain ranges hosting anomalously high levels of CO_2, and basin regions hosting lows. The cause of these tendencies has not been determined. Calculations applied to the OCO-2 instrument, scheduled for a 2013 launch, found that it will be capable of detecting the coal plant's emission and may be a viable tool for detecting large carbon leaks from sequestration sites.

Introduction

The global mean temperature of the Earth's surface and atmosphere has been shown, through multiple data sources and metrics, to have increased over the past century, and the decade of 2000-2009 was the warmest decade on record since 1880 [NCDC, 2011]. Multiple paleoclimatic studies have also demonstrated that recent decades were warmer than any other period in the past two millennia. This pattern has been tied in part to the continuing increase of carbon dioxide (CO_2) concentration in the atmosphere. Global carbon output and average global temperature, correspondingly, are predicted to increase substantially over the 21st century. Decreasing the total anthropogenic CO_2 output may significantly mitigate the effects and severity of future climate change [IPCC, 2007].

Carbon capture and geologic sequestration is a potential, though not currently widespread, method of reducing total atmospheric carbon. In this method, CO_2 is filtered from industrial/power plant emissions and injected into a subsurface geologic formation capable of storing carbon. This approach can apply to coal seams and other porous formations, in which the carbon chemically and structurally affixes to the surrounding rock, and saline aquifers, in which carbon dissolves. In conjunction with carbon scrubbing techniques, sequestration could significantly mitigate the emission of carbon-burning power plants. Scrubbing and sequestration could reduce the carbon output of a given carbon-fired plant by 80-90%, and the geologic carbon storage capacity in the US alone is large enough for capture and sequestration to be a long-term (100+ year) method of emission reduction [Plasynski, 2011]. Although

properly selected sites are predicted to maintain nearly all of their input carbon even over large time scales, the possibility exists for CO_2 migration and eventual leaking [Holloway, 1997]. In addition to local methods of carbon leakage monitoring, such as flux towers [Lewicki et al., 2010] and monitoring of local vegetation health [Male et al., 2010], remote methods could be a significant asset to leak detection at sequestration sites. Orbital instruments in particular would be capable of instantaneous sampling of large areas with high time frequency, enabling regular monitoring of a sequestration region without the need for multiple, individual ground sites. After the initial launch investment, data collection and analysis would be inexpensive.

Our project tests the potential applicability of two orbital instruments to methods of detection of regional increases in atmospheric CO_2 concentration: The SCanning Imaging Absoprtion spectroMeter for Atmospheric CHartographY (SCIAMACHY) and the Greenhouse gases Observing SATellite (GOSAT). GOSAT was launched by the Japan Aerospace Exploration Agency (JAXA) on January 23, 2009 on a five year mission, and is designed to measure atmospheric column densities of CO_2 and methane (CH_4) via a Fourier Transform Spectrometer (FTS) [Hamazaki, 2005; Butz et al., 2011]. SCIAMACHY is a spectrometer aboard the European Space Agency's ENVISAT satellite, launched in March 2002, and measures total column densities for CO_2 using the WFM-DOAS retrieval algorithm, which has been improved several times over the course of its mission [Bovensmann et al., 2010a]. This project used data from the v2.0 algorithm.

Monitoring carbon dioxide (CO_2) leaks from sequestration sites globally is critical to the viability of carbon sequestration as a method of reducing atmospheric CO_2. Subsurface carbon sequestration within a geologic medium is considered an important tool in offsetting rising levels of atmospheric CO_2 [Reiche et. al., 1999; Figuerora et al., 2008]. Remote sensing of emissions and associated atmospheric plumes can be challenging due to the high variability of natural CO_2 in the atmosphere [Olsen and Randerson, 2004]. This study considered instrument response and sensitivity, potential geospatial methods for point source and plume detection, geostatistical and data aggregation methods, and large-scale natural concentrations of CO_2 in the atmosphere associated with topography. The viability of potential methods of detection and monitoring hinges on the sensitivity of the observing instruments.

We tested these methods using CO_2 column readings near geographically isolated, high-volume anthropogenic point sources. Geospatial and geostatistical methods include time series analysis, comparative measurement across distance from the source, anomaly and plume mapping, and analysis and data aggregation by wind directionality relative to the source. Large-scale, seasonal patterns of CO_2

distribution as measured by SCIAMACHY were found using Kriging interpolation of data collected over the continental US. The estimated theoretical sensitivity of GOSAT, SCIAMACHY, and the future OCO-2 instruments to CO_2 point sources were calculated using the absolute CO_2 sensitivity and measurement footprint size of each instrument.

Background

The cumulative effect of industrialization has increased the global atmospheric CO_2 concentration from 280 ppm in 1750 to 392 ppm in 2011, with a global average temperature increase of ~ 1°C since 1850 [IPCC, 2007; NCDC, 2011]. The IPCC forecasted a continuation of the global warming trend through the 21st century, with a predicted total increase in global average surface temperature between 1.5° and 6.1° C, depending on the quantity of future carbon emission. This sharp change in atmospheric temperature is likely to have serious ramifications on human welfare and the natural environment through sea level rise and shifts in weather patterns. Some regions may become more susceptible to drought or flooding, and heavily populated, low-laying coastal regions will become especially vulnerable to surge flooding. Emission mitigation efforts, if widely applied, will reduce the amount and impact of future warming [IPCC, 2007]. Carbon capture and storage is capable of reducing the CO_2 output of electric and industrial plants, which are responsible for about a third of the total US emission, by 80-90%.

Geologic carbon sequestration is the process of injecting supercritical liquid carbon dioxide, filtered and isolated from the emissions of industrial and electric plants, into a geologic medium capable of retaining the carbon. Typical locations for storage are coal seams and gas and oil wells, in which the carbon chemically and structurally affixes to the surrounding rock, and saline aquifers, in which carbon would dissolve. Sequestration in partially depleted oil and gas wells is particularly economical, as the displacing action of carbon injection aids the extraction of oil and gas. Similarly, injection into coal seams displaces the methane gas commonly contained in these formations. Both of these methods, properly applied, may provide a low net cost method of emission reduction in the power-generation sector [IPCC, 2005; Plasynski, 2011]. In the US, oil, gas, and coal reservoirs have an estimated storage capacity of 316 gigatonnes (Gt, 10^{12} kg), which at current estimated US point source emission rates would provide 83 years of complete CO_2 storage. Storage in saline formations, though without an intrinsic economic gain from carbon injection, would provide storage capacity for 867-3320 additional years at the current rate of emission [Plasynski, 2011].

Monitoring of CO_2 behavior in sequestration sites after injection is a crucial part of the overall process. In addition to reducing the efficacy of the carbon storage method, leakage could have detrimental effects on vegetation and water resources. This possible effect on water quality brings sequestration methods under the purview of the Underground Injection Control (UIC) Program of the United States Safe Drinking Water Act, which further solidifies the demand for a wide variety of monitoring methods [Plasynski, 2011; Little, 2010]. Potential methods for monitoring include well analysis via boreholes and seismic sensors, soil sampling, local atmospheric sampling via eddy covariance towers, and aircraft-borne LIDAR measurements [Bateson et al., 2008]. DOE field studies in North Dakota and Kentucky have demonstrated that vertical seismic profiling and microseismic surface measurement will be capable of monitoring the plume behavior of the well as a whole, for oil/gas/coal wells as well as saline formations .Though this is a crucial level of well monitoring, it would not directly sense surface leakage [Plasynski, 2011]. Eddy covariance towers have been shown to provide this with some limitations [Miles, 2005]. Depending on atmospheric conditions, leak detection may be delayed or misidentified, and its effect is strictly local. This general result was duplicated at a controlled release test site in Montana [Spengler et al., 2009]. The Montana tests show encouraging results for laser-based instruments as well, although these and eddy flux instruments are similarly limited to strictly local measurement, making them best suited for detection of leakage at the injection point itself. Across larger regions of sequestration, a wider method of aerial CO_2 detection is needed. We tested the ability of orbital remote sensors (SCIAMACHY, GOSAT, and, theoretically, OCO-2) to fill this need.

ENVISAT's SCIAMACHY instrument is capable of quantifying the spectral absorptions and column densities of O_3, NO_2, OClO, H_2O, SO_2, BrO, and CO, and can also measure cloud cover and cloud optical thickness. It uses the unique Full Spectral Initiation Weighting Function Modified Differential Optical Absorption Spectroscopy (FSI WFM-DOAS) algorithm applied to its NIR Nadir sensor to estimate CO_2 column ratios in ~30×60 km ground swath footprints. ENVISAT's orbital pattern is repeated every 35 days, though taking full swath width into account the globe is covered over 2-3 days. Cloud cover and aerosol measurements are used to flag the quality of each reading, where data flagged as "bad" are discarded. Practically, the highest concentration of "good" SCIAMACHY CO_2 measurements on the ground occurs between 15° and 30° latitude (Figure 1). The SCIAMACHY data used in this project was calculated using the WFM-DOAS v2.0 algorithm. This version of the data was tested against CarbonTracker data in 2010 by the University of Bremen [Schneising et al., 2010]. CarbonTracker is a global predictive model of CO_2 based on a wide array of NOAA CO_2 ground measurements. The increase

in annual mean carbon ratio over this time span was measured as 1.8±0.13 ppm for SCIAMACHY and 1.8±0.09 ppm for CarbonTracker. The amplitude of global seasonal CO_2 change for SCIAMACHY and CarbonTracker was 2.8±0.2 ppm and 1.7±0.1 ppm, respectively. This discrepancy in seasonal amplitude measurement was attributed to a noted underestimation of net ecosystem exchange in the CarbonTracker model. WFM-DOAS v2.0 data has also been tested against local, ground-based FTS and Total Carbon Column Observing Network (TCCON) sensors [Reuter et al., 2011]. SCIAMACHY was shown to have a standard error of 0.2-0.8 ppm, with a single measurement precision of 2.5 ppm. The FTS/TCCON and SCIAMACHY data was also compared against CarbonTracker. The site in Darwin Australia showed CarbonTracker having lower winter estimates than both methods, suggesting that the discrepancy in seasonal amplification between SCIAMACHY and CT observed in the ealier study was largely due to CT's underestimation.

GOSAT, launched in January 2009, is a joint venture of the National Institute for Environmental Studies (NIES), the Japanese Space Agency (JAXA) and the Ministry of the Environment (MOE), carrying the Thermal And Near-infrared Sensor for carbon Observation Fourier Transform Spectrometer (TANSO - FTS) [Hamazaki, 2005]. Concurrent measurements are taken by a second, NIR-Thermal sensor, designed to detect cloud and aerosol cover at the location of the FTS CO_2/ CH_4 measurements, and through this the quality of the column measurements are classified. CO_2 column measurements have a nadir footprint of 10.5 km, with an orbital repeat cycle of three days. It uses a wide, flexible, sweeping scan pattern capable of sequentially testing regions within ±35° (~750km) of the nadir track [Boesch et al., 2011]. Tested against 6 TCCON sites, GOSAT measurements had a root mean standard deviation of 2.8 ppm [Butz, A., et al., 2011].

OCO-2, due for an early 2013 launch, is being developed by JPL for the specific purpose of regional CO_2 source/sink analysis. OCO-2 is a refinement of the OCO satellite, which failed during launch in 2009. OCO was designed for high spatial precision CO_2 detection, and was considered potentially capable of detecting surface carbon fluxes, such as emission from landfills [Vigil and Crisp, 2010]. OCO-2's goals are 1-2 ppm XCO_2 sensitivity with nadir-mode measurements taken over a 3 km^2 footprint, with 10km swath width. This relatively small footprint size will have the effects of increased data density (fewer regions will be invalidated by partial cloud cover) and increased sensitivity to point source carbon (sources will have a greater impact on the carbon ratio of thinner columns). It uses a unique algorithm, the OCO Full Physics Retrieval Algorithm, originally designed for the OCO satellite [Boesch et al, 2011]. Before the launch of the OCO satellite, this algorithm was tested using the SCIAMACHY sensor against

ground FTS readings in Wisconsin, showing the SCIAMACHY data with a positive bias of ~3.5% versus the FTS. This was seen as a successful proof of concept for the algorithm, given that it's designed for much greater spatial resolution than SCIAMACHY can provide [Bösch, H., et al., 2006]

The University of Bremen is now developing a satellite designed with CO_2 and CH_4 point source detection specifically in mind: The Carbon Monitoring Satellite, or CarbonSat. This satellite is one of two candidates for the European Space Agency's Earth Explorer 8 launch in 2018 [Bovensmann, H., et al, 2010b]. CarbonSat would have a 4 km^2 footprint with a 500km swath width, with a <1ppm precision in carbon ratio. This is projected to produce an average of 6,440,000 cloud free measurements daily (in comparison to 453600, 3500, and 1300 for OCO, SCIAMACHY, and GOSAT respectively). The resulting high data density should increase the viability of CO_2 plume mapping techniques for emission detection [Bovensmann, H. et al, 2010c; Burrows, J.P. et al., 2010].

Methods

Leaks from carbon sequestration facilities will manifest as a point source increase in atmospheric CO_2, which through a combination of atmospheric diffusion and wind velocity, will extend the zone of this CO_2 in an outwardly expanding plume. Four-dimensional variations in plume geometry will occur as a result of wind variability with time and atmospheric elevation. The overall plume geometry is expected to result in an xCO_2 signal that both decreases and widens with distance from source. The detection of a point-source emission or the resulting plume is dependent on (1) instrument sensitivity; (2) atmospheric affects; (3) topographic influence; (4) spatial and temporal resolution; and (5) data density. Beyond elevation effects related to density of the atmospheric column, topographic influence is poorly understood with respect to constraining atmospheric CO_2 [Pillai, D., et. al., 2010]. Natural variability of the system and poor spatial and temporal coverage constrain the development of geospatial approaches to detect point-source emission on the Earth's surface similar to a sequestration leak. We evaluated current feasibility of using data from existing space-borne assets, GOSAT and SCIAMACHY, and considered the potential application to data from the yet to be launched OCO-2 to detecting CO_2 point source emissions on the Earth's surface.

As proxy for a point-source sequestration leak, we targeted coal-fired electrical generation plants, isolated from major urban areas. These were chosen to ensure a large CO_2 signal and to limit the

input of other anthropogenic sources. Targeting was also influenced by the temporal and spatial availability of data from GOSAT and SCIAMACHY orbital platforms. The Jim Bridger Power Plant in Wyoming meets these targeting criteria and was chosen for study. The objective was to evaluate the potential for leak detection, as well as to develop geospatial methods that could identify and locate point source emissions of CO_2.

We considered a number of geospatial methods to identify and monitor leaks using space-borne assets. We used existing SCIAMACHY data from 2005 **and earlier** in testing geospatial approaches to detecting point-source emissions. These include:

1. Time series anomaly detection of target and immediately adjacent areas
2. Anomaly mapping
3. Plume detection using transects orthogonal to local wind directions

Time Series Anomaly Detection

To test geospatial approaches capable of ongoing monitoring of potential point-source emissions we chose the Jim Bridger plant in southwestern Wyoming for its high emission (15.8 Mt of CO_2 in 2006 [EIP, 2007]), isolated and undeveloped location, semi-arid environment, and availability of local SCIAMACHY data points over the summer 2005 (Figure 2). The high-emission CO_2 point source of Jim Bridger and the relative lack of additional anthropogenic sources in the surrounding region provide a clear demonstration of how a local CO_2 point source of this magnitude would register in a SCIAMACHY dataset. The core logic behind our geospatial methods for testing SCIAMACHY's sensitivity to CO_2 point sources (in this case, Jim Bridger) was comparison between measurements taken near the source and those located farther from its influence. These could be compared in time series or evaluated independently. Our methods were designed to be used with general coverage data from a space-borne instrument with sufficient sensitivity to detect local CO_2 anomalies related to point source emissions and resultant plumes**.**

In analyzing the Jim Bridger region, our basic objective was to detect and qualify the carbon signal from the emission source, as it appears in SCIAMACHY data, of the surrounding area. Our first test of Jim Bridger's local impact was a comparison of the CO_2 readings of two sub-regions: the area within a 20 mile radius of the plant, and a control region of the same size roughly 80 miles to the east (Figure 3). From these two zones we selected data for which a corresponding measurement had been taken on the

other zone on the same date. In this way we plotted and compared concurrent readings near and away from the Jim Bridger plant over the season (Figure 4). We would expect a detected CO_2 signal from Jim Bridger to appear as more-or-less consistently higher CO_2 readings above the plant relative to the control zone.

To account for the possible influence of directionality and wind, we used the same method of gathering and comparing readings within circular zones of 20-mile radius over time, using 5 circles: One centered on the plant, and four located adjacently in the cardinal directions. We plotted these readings (Figure 5) alongside the daily average wind direction over the summer, taken from the weather station at Point of Rocks, roughly five miles south of Jim Bridger. Where more than one reading from a given day was located within a circle, we plotted the higher reading looking for a signature of the source and associated plume.

Localized emissions and associated plumes of CO_2 should be seen as anomalies compared to adjacent areas over time. Time series mapping of anomalies given low data density and temporal coverage may not be sufficient to recognize a point-source emission and/or resulting CO_2 plume. The xCO_2 measurements in the vicinity of the Jim Bridger power plant during the summer of 2005 indicate high intra-seasonal variability (see Figure 5).

Spatial Anomaly Detection

Low data density for any specific set of continuo usly obtained xCO_2 measurements make direct anomaly mapping problematic. We have considered several methods to increase data density through geostatistical and data aggregation methods.

Geostatistical methods include analysis of interpolated data and grid-cell averaging, while data aggregation includes time-concurrent or parameter-selective multi-orbital combinations of observed xCO_2. Given the high temporal variability of the xCO_2, unrestricted multi-orbital aggregation seems problematic in application. We tested selective filters including time dependent (aggregating data within a two-week period) and wind dependent (aggregating data based on wind direction during observation) against the data as a prerequisite to aggregation.

One method considered “binned” data over summer 2005 depending on local wind patterns. In this method data over the season is aggregated into bins depending on wind direction. For example, a

measurement located SE of the plant when the wind was blowing SE would be in the same bin as a measurement located NE of the plant when the wind was blowing NE. The initial analysis was done with 5° bins for prevailing winds. A general comparison of data selection over the three month period based on wind directions can be seen in Figure 6 below. Wind bins of ever increasing angular windows were evaluated to consider trade-offs between increased data density, xCO_2 resolution, and temporal variability.

Plume Detection

Temporal variability of xCO_2 data is not a factor in using transects of data crossing the direction of prevailing winds if we only use data from a single scan. The objective of this method is to cross the plume generated from a point source and carried downwind. Presumably, higher levels of CO_2 will be detected across the axis of a plume and a number of parallel transects could be used to characterize the orientation of the plume and its source. A number of transects, showing xCO_2 concentrations against distance to the center point of the sampling region, were constructed roughly orthogonal to the prevailing winds. Examples of transects in the Jim Bridger area are shown in Figure 7. Ideally, data density would be high enough to use a number of parallel transects to map the plume from the point source outward in the direction of prevailing wind. This method uses only data collected from a single orbital pass and therefore eliminates potential temporal variability, but it may still be subject to larger-scale natural variability in the atmospheric system.

To consider the larger-scale context and framework for our localized study around the Jim Bridger Power Plant, we examined patterns of SCIAMACHY data on the continental scale. We interpolated the 26,600 data points collected within the contiguous US over June-August 2005, using the Kriging method of spatial interpolation packaged in ArcMap's Spatial Analyst extension (Figure 8). Kriging is a linear least squares reduction method that was designed for mapping trends in randomly sampled data through use of semivariogram modeling [Johnston, et. al., 2001]. As applied to our data, Kriging provides a clear look at some of the dominant spatial patterns of SCIAMACHY's CO_2 readings. The data was interpolated using Ordinary Kriging and a spherical Semivariogram, producing a raster with a 0.1 degree cell size. Each cell value is based on the 32 nearest data points. The data interpolation allowed for a context to consider potential natural long-term spatial variability of expected values that may affect the application of localized methods to study point source emissions.

Calculation of theoretical CO_2 sensitivity of GOSAT, SCIAMACHY and OCO-2

The methods proposed in this study are limited by the sensitivity of the instruments to observe CO_2 sources and resultant plumes. To obtain a first-order estimate of how large a CO_2 source must be to be detectable by GOSAT, SCIAMACHY, or OCO-2, we began by calculating the amount of excess CO_2 mass that must be in the atmospheric footprint of each satellite to increase the CO_2 concentration within that footprint by 1 ppm. Here, the atmospheric footprint refers to the entire volume of atmosphere within each instrument's field of view, neglecting any motion of the atmosphere that occurs during the sub-second exposure times typically used during observations.

Because the overall density of the atmosphere decreases as elevation increases, less additional CO_2 mass will be needed to raise the concentration of CO_2 by 1 ppm at higher elevations. For heights up to 80 km, atmospheric density can be approximated as an exponential decay:

$$\rho_{air} = \rho_0 \times 10^{-\tau z}. \qquad (1)$$

Here, ρ_{air} is the density of the atmosphere as a function of elevation, z, in m, atmospheric density at sea level, ρ_0, in kg m^{-3}, and a decay constant, τ, in m^{-1}. Beyond 80 km elevation, atmospheric density is negligible, and we ignored it in our calculation.

We numerically integrated the volume of each instrument footprint as a series of thin cylinders (GOSAT) or rectangular prisms (SCIAMACHY, OCO-2). That is, volume of a given slice, V_z, is given by:

$$V_z = (1/2 \times FOV \times (A_{sat} - z))^2 \times \pi \times \Delta z, \qquad (2)$$

for GOSAT, and:

$$V_z = (FOV \times (A_{sat} - z))^2 \times \Delta z, \qquad (3)$$

for SCIAMACHY and OCO-2. In these equations, FOV is the angular field of view of the instrument, in radians. Note that Equation 3 assumes that the across-track and along-track fields of view are the same for SCIAMACHY and OCO-2. This assumption is wrong, but the difference should be negligible for our purposes. Additionally, A_{sat} is the average orbital altitude of the satellite, in m, and Δz is the elevation increment used for numerical integration, in m. Each volume increment was then multiplied by the

density of the atmosphere at that elevation to obtain a mass increment, M_z, and the mass increments were added together for the atmosphere in between the satellite and the surface of the Earth f or some surface elevation, H, to get the total atmospheric mass within the instrument footprint, M_{total}. That is,

$$M_z = \rho_{air} \times V_z, \quad (4)$$

and,

$$M_{total}(H) = \sum_{z=H} M_z. \quad (5)$$

Here, the summation occurs over elevations ranging from the surface elevation to 80 km. Repeating this calculation for a range of surface elevations provided M_{total} as a function of surface elevation. We then divided this total mass by 10^6 and multiplied by the ratio of CO_2 molar weight to dry air molar weight, μ, to obtain the excess mass of CO_2 needed to raise the concentration of CO_2 in the atmospheric footprint of the instrument by 1 ppm. That is, the mass of CO_2, in kg, needed to increase the concentration within the atmosphere contained by the footprint of the instrument by 1 ppm, C, as a function of surface elevation, H, is given by

$$C(H) = \mu \times 10^{-6} \times M_{total}(H). \quad (6)$$

For all calculations we used

$\rho_0 = 1.2$ kg m^{-3},

$\mu = 1.5$,

$\tau = 5.81 \times 10^{-5}$ m^{-1},

$\Delta z = 100$ m.

The results of this calculation for GOSAT, SCIAMACHY and OCO-2 are shown in Figure 9. For GOSAT, we used FOV = 0.0158 radians, and A_{sat} = 667,000 m. Similarly, for SCIAMACHY we used FOV = 0.0314 radians, and A_{sat} = 800,000 m. For OCO-2, we used FOV = 0.0016 radians, and A_{sat} = 705,000 m.

Knowing the amount of CO_2 needed to increase the atmospheric footprint by 1 ppm, we can compare this number to the amount of CO_2 we expect to be found within the same footp rint due to sources of various size. For example, Jim Bridger Power Station produces ~43 kt CO_2 per day during normal operation. This is equivalent to ~500 kg s^{-1}. Jim Bridger Power Station is located in Wyoming, which is a windy place. For this calculation, we assume average wind speed is 5 m s^{-1} (about 10 mph). Thus, over 1 s, 500 kg CO_2 will be spread over 5 m in the direction of the wind, creating a plume with CO_2

linear mass density of 100 kg m^{-1}.

The nominal footprint size on the Earth's surface is 10 km for GOSAT, 30 km for SCIAMACHY, and 1.6 km for OCO-2. If the plant is located in the center of an instrument footprint, then we can expect 5×10^5 kg excess CO_2 in a GOSAT footprint due to the power plant, 1.5×10^6 kg in a SCIAMACHY footprint, and 8×10^4 kg in an OCO-2 footprint.

The surface elevation at Jim Bridger Power Station is about 2 km. Examining Figure 9, we find that 9×10^5 kg CO_2 are needed to raise the concentration in a GOSAT footprint by 1 ppm. Thus, we can expect Jim Bridger Power Station to result in a 0.56 ppm "signal" for GOSAT, ignoring instrument precision. Similarly, SCIAMACHY needs 6.5×10^6 kg and OCO-2 needs 1.3×10^4 kg for a 1 ppm increase. Thus, we expect the plant to produce a 0.23 ppm "signal" for SCIAMACHY and a 6.2 ppm "signal" for OCO-2. The precision of SCIAMACHY measurements, however, is ~2.5 ppm [Reuter et al., 2011], or 10 times greater than the expected signal from Jim Bridger Power Station.

In general, for a given source flux, F, in kg s^{-1}, a wind speed, W, in m s^{-1}, a linear pixel size, Δs, in m, and C(H), given by Equation 6, we can calculate a detection ratio, D, at a given surface elevation, H, given by

$$D = (F \times \Delta s) \div (W \times C(H)), \quad (7)$$

where

$$\Delta s = FOV \times (A_{sat} - H), \quad (8)$$

and D = 1 corresponds to a 1 ppm increase. Here we assume that the source is located at the edge of a pixel, with the plume passing through the entire footprint. Rearranging Equation 7, we can assign a detection threshold, e.g. D = 3 ppm, in order to estimate the minimum flux detectable by an instrument as a function of wind speed and surface elevation:

$$F = (D \times C(H) \times W) \div \Delta s. \quad (9)$$

Note that $C \sim (\Delta s)^2$, thus $F \sim \Delta s$. The results of Equation 9 for OCO-2 are shown in Figure 10. We neglected atmospheric diffusion processes, but for this reason we did not calculate F for wind speeds below 1 m s^{-1}.

Analysis

Our study of the coal-fired Jim Bridger Power Station in Wyoming illustrates the challenges of detecting CO_2 point-source emissions from orbital platforms. Existing assets considered in this study (GOSAT and SCIAMACHY) apparently lack the sensitivity to pick up even the relatively large point-source emissions generated at this facility (~43 kt CO_2 per day [EIA, 2005]). Additionally, GOSAT spatial coverage does not allow for the data density required to practically apply the detection methods tested in this project. SCIAMACHY data allows for application of various geospatial and aggregation methods to look for point-source emissions of CO_2 and their resultant plumes, but lacks the sensitivity and resolution to detect the signal of even a large coal-fired power plant. The inability to consistently see higher xCO_2 concentrations in and around the Jim Bridger Power Plant (Figures 4 and 5) is apparently related to the low signal response.

Figure 4 compares the xCO_2 of the two sub regions over time, between 6/19/2005 and 8/28/2005. During that time period there are four dates (6/22, 7/23, 7/30, and 8/27) with significantly higher on-plant XCO_2 readings versus those to the east. However, there is not a consistent pattern of higher values occurring on the plant, and there are dates when the control zone registers as higher, albeit not to the same degree of the four spikes observed in the region on the plant on other days. We would expect a CO_2 signal from Jim Bridger to appear as higher CO_2 readings above the plant relative to the control zone.

To account for interference from atmospheric flow in the near surface, we compared five subareas, each with a 20-mile radius, with one centered on the plant and the other four in cardinal directions. A plot of the xCO_2 values over time and a plot of average wind direction over the same time period show no consistent signal over the plant (Figure 5). Southwesterly winds are dominant for a large majority of the season. However, no directional zone is consistently higher than the others. The spikes in on-plant CO_2 versus those to the east are still evident, but the noisiness of this greater dataset suggests against a consistent signal from the plant source. It may be worth noting that the western zone (which should theoretically have less CO_2 input from the plant, relative to other zones) contains the lowest reading for all but two dates. However, 7/30 contains a spike in the western zone far exceeding the day's values for the plant zone and the eastern zone, despite a consistently westerly wind for the local time frame. The variability of these results suggests factors beyond pure wind effect, possibly topographic variances within each circular zone.

We also plotted each xCO_2 value centered within 100 miles of the Jim Bridger plant (Figure 2) as xCO_2 by distance over time (Figure 11). This plot shows no correlation between proximity to the plant and CO_2 level, and shows that CO_2 values are more correlated with time than they are with location relative to Jim Bridger. To check for wind bias, we also plotted this data as distance vs. azimuth from the plant (Figure 12), which shows no correlation. This lack of correlation between CO_2 and distance or direction suggests that the point source, Jim Bridger, does not have a significant impact on xCO_2 observable with SCIAMACHY relative to daily weather conditions. Though some differences seem to persist, for a point source with an expanding plume in a steady-state high xCO_2 concentrations should be discernible in a direction downwind. Detection of a plume related to a point source is more likely with tightly constrained binning of data with respect to wind directions.

A general comparison of data selection based on wind directions can be seen in Figure 6. Aggregating data over the season for prevailing wind, by combining observations from days in which wind directions were similar, allowed for an increase in the density of the data relative to the source. If winds have significant impact on plume location and geometry, then aggregating data by this method may help determine the location of an original point source. This wind binning method was tested with varying results depending on initial data density. Bin sizes vary from 5° to 50° and temporal aggregation of one to three months were tested. Figure 13 shows an example of a map generated through wind binning, aggregating xCO_2 data sampled for winds varying from 260° to 265° during the summer of 2005. This map generally shows higher xCO_2 values in the vicinity of Jim Bridger and dropping slightly to the east away from the prevailing winds. Values west of Jim Bridger on the Westside of the ridgeline in the area of North Rock Springs are significantly lower. Given the low data density it is not clear whether this represents a signal from the Jim Bridger Power Plant. Lowering the bin sizes significantly reduces the enhancement of data density, while increasing the number of distinct time periods over which data was collected. Aggregation still seems to be problematic given the high temporal variability in collected data. Wind binning as a method for aggregating data seems a viable approach given sufficient instrument sensitivity. This method also aggregates the signals from associated plumes, widening their footprint with increasing bin size.

To detect plumes directly from data a series of parallel transects were constructed from xCO_2 data roughly perpendicular to the average wind direction (Figure 7).The two parallel transects intersect a localized xCO_2 high that is sub parallel to the direction of the prevailing wind. The source of the high is

most likely independent of the Bridger plant, but it demonstrates the strength of the approach. A series of roughly parallel transects,, given initial data density, could be used to roughly define the geometry and limits of a CO_2 plume. This method, like the others discussed above, could be used with data density similar to the current SCIAMACHY data set but would require greater sensitivities to look at the CO_2 anomalies potentially encountered by a sequestration leak.

In the analysis of localized data sets around the Jim Bridger Power Plant, the absence of a strong anthropogenic signal has brought into focus the high natural variability of CO_2 regionally. We examined spatial variability of xCO_2 from SCIAMACHY data available for the continental United States. Using a standard Kriging method to interpolate the data we examined spatial variability of CO_2 for the same summer months of 2005 (Figure 8). The interpolated map does not show influence from coal plants or any other anthropogenic source. However, it does show some strong relationships between CO_2 and topography, of which we have not found a clear cause. Most prominent is the tendency for fields of high CO_2 to be found on the east flanks of mountain ranges, especially in the western mountainous regions. This effect can be observed throughout the western U.S. Some notable examples have been circled in Figure 14, including the Klamath and Sierra Nevada ranges, the Sierra Madre, and several fronts of the Rocky Mountains. Figure 15 also shows examples of the tendency for basins to maintain low CO_2 readings. This tendency is especially noteworthy in the case of California's Central Valley, which has consistently very low values despite its high population and transportation sector. The strong contrast seen on both flanks of the Sierra Nevada seems to suggest a relationship between these two trends, though the Snake River and Columbia basins also show the low pattern without a clear association with a mountain range high.

Transects along mountain ranges in the western U.S. show the same correlations across the crest of the Sierra Nevada (Figures 16 and 17). Comparison of the data along the transect shows that xCO_2 highs exist just east of the crest of the Sierras along the leeward slopes and corresponding lows are offset from the basin axis of the Central Valley along the western windward slopes. A similar phenomena was measured by the NASA Ames Research Center Alpha Jet while flying a transect from Moffett Field, California to Railroad Valley, Nevada on June 26, 2011. CO2 , CH4 and H20 were measured with a cavity ring-down spectrometer [Olson, et. al., 2011]. The measurements showed a peak in CO2 concentrations along the eastern slope of the Sierras at longitude 118 degrees west.

This pattern is repeated across the Klamaths, Cascades, and parts of the Coast Ranges. The analysis of this data suggest atmospheric topographic interactions that are poorly understood and may impact future, more localized or regional investigations of anthropogenic point-source emissions of CO_2.

Discussion and Conclusions

We have developed a method to determine the limits of sensor resolution. Using this method, we estimated that the minimum observable point source for OCO-2 under reasonable wind conditions (2.5 m s^{-1}) will be ~8 kt/day. Thus, OCO-2 may be able to detect point source leaks from sequestration sites, provided the leak rates are large, similar in output to a small coal-fired power plant. Using the sensor in targeted mode, which should provide greater sensitivity (precision), will allow it to detect smaller leaks than this. The above calculation, for instance, assumes sensor precision of 3 ppm. Since our estimate considers sensor precision as a linear factor, improving precision to 1 ppm implies OCO-2 may be able to detect a point source ~2.3 kt/day. In order to detect a leak on the order of 1 kt/day, a sensor with 1 ppm resolution would need ~800 m resolution.

From a monitoring perspective, leaks from sequestration sites will likely be easier to detect when the sites are located between 15° and 30° latitude (Figure 1) at high elevation and with low average wind speeds, although wind speed is a much more important factor. Additionally, xCO_2 values appear to be lower, on average, in basins such as California's Central Valley (Figure 15), which would suggest these locations will have lower background noise levels.

The point-source and resulting plume may be detected and monitored over time using various geospatial approaches. Data from GOSAT and SCIAMACHY instruments were evaluated relative to these approaches and found to have serious limitations in practice due to low sensitivity and temporal and geospatial data density. Instrument sensitivity with respect to atmospheric column measurements of xCO_2 is the more problematic consideration and could not be overcome by geostatistical methods. Instrument specifications for the future orbital sensors OCO-2 and CarbonSat, however, indicate that atmospheric column data of xCO_2 may allow for the application of these methods and approaches.

The simplest approach to detection of a point-source emission anomaly is comparison of data gathered in and around a target site in time series. Currently available data from GOSAT and

SCIAMACHY does not have the coverage to allow for this direct approach. Targeting operations of a satellite instrument, with sufficient sensitivity, over a site on repeated days could detect the presence of an emission. This would require deliberate targeting of a suspected site, but is inefficient for the ongoing monitoring of multiple sites across large regions.

References Cited

Bateson L, Vellico M, Beaubien SE, Pearce JM, Annunziatellis A, Ciotoli G, Coren F, Lombardi S, Marsh S., 2008, The application of remote-sensing techniques to monitor CO_2-storage sites for surface leakage: method development and testing at Latera (Italy) where naturally produced CO_2 is leaking to the atmosphere. Int. J Greenhouse Gas Control 2:388–400

Bovensmann H., Buchwitz M., Burrows , J. P., Reuter M., Krings T., Gerilowski K., Schneising O., Heymann J., Tretner A., and Erzinger J., 2010a. A remote sensing technique for global monitoring of power plant CO_2 emissions from space and related applications. Atmos. Meas. Tech., 3, 781–811

Bovensmann H., Buchwitz M., Burrows , J. P., 2010b. Greenhouse Gas Satellite Mission CarbonSat Selected by European Space Agency ESA. Press Release, University of Bremen, November 2010.

Bovensmann H., Buchwitz M., Burrows , J. P., 2010c. Carbon Monitoring Satellite as an Earth Explorer Opportunity Mission: Mission Overview. University of Bremen, June, 2010.

Burrows J.P., Buchwitz M., Bovensmann H., Schneising O., and Reuter, M., 2011. Passive Satellite Remote Sensing Methane and Carbon Dioxide: From SCIAMACHY towards CarbonSat and CarbonSat Constellation. University of Bremen.

Boesch, Baker, Connor, Crisp, Miller, 2011. Global Characterization of CO_2 Column Retrievals from Shortwave-Infrared Satellite Observations of the Orbiting Carbon Observatory -2 Mission. Remote Sens., 3, 270-304.

Bösch, H., Toon, G. C., Sen, B., Washenfelder, R.A., Wennberg, P.O., Buchwitz, M., de Beek, R., Burrows, J. P., Crisp, D., Christi, M., Connor, B. J., Natraj, V., Yung, Y. L., 2006. Space-based near-infrared CO_2 measurements: Testing the Orbiting Carbon Observatory Retrieval Algorithm and validation concept using SCIAMACHY observations over Park Falls, Wisconsin. Journal of Geophysical Research, Vol. 111, D23303, doi: 10.1029/2006JD007080.

Butz, A., et al., 2011. Toward accurate CO_2 and CH_4 observations from GOSAT, *Geophys. Res. Lett.*, 38, L14812, doi:10.1029/2011GL047888.

Environmental Integrity Project, July 2007. Dirty Kilowatts: America's Most Polluting Power Plants, U.S. Department of Energy, Washington, DC.: 65 pp.

Energy Information Agency (EIA), 2005, EIA-923 Monthly Time Series File, U.S. Department of Energy, Washington, DC.: 1947 pp.

Figueroa J., Fout, T, Plasynski M, McIlvried H. Rameshwar D. Srivastava, R., 2008. Advances in CO_2 capture technology—The U.S. Department of Energy's Carbon Sequestration Program. Int. J Greenhouse Gas Control 2:9–2 0

T. Hamazaki, 2005. GOSAT Project and Mission Overview, 12th ASSFTS (Atmospheric Science from Space using Fourier Transform Spectrometry) Workshop, Quebec City, Canada.

Holloway, S. 1997. Safety of the underground disposal of carbon dioxide. Energy Convers. Manage. 38(Suppl.) S241–S245.

Intergovernmental Panel on Climate Change, 2005. Chapter 5: Underground Geological Storage. IPCC Special Report on Carbon Dioxide Capture and Storage, 197-264.

Intergovernmental Panel on Climate Change, 2007. IPCC Fourth Assessment Report (AR4). Summary for Policymakers. Geneva, Switzerland.

Johnston, K., Ver Hoef, J, Krivoruchko, K., and Lucas, N., 2001. Using ArcGISTM Geostatistical Analyst: ESRI,

Redlands, California, 301 pp.
Little, M., Jackson, R., 2010. Potential Impacts of Leakage from Deep CO_2 Geosequestration on Overlying Freshwater Aquifers. Environ. Sci. Technol., Vol. 40, No. 30.
Male, E. J., Pickles, W.; Silver, E.; Hoffmann, G., Lewicki, J., Apple, M., et al., 2010. Using hyperspectral plant signatures for CO_2 leak detection during the 2008 ZERT CO_2 sequestration field experiment in Bozeman, Montana, Environ Earth Sci (2010) 60:251–261
Miles, L., Davis, K., Wyngaard, C. 2005. Using Eddy Covariance to Detect Leaks from CO_2 Sequestered in Deep Aquifers. Pennsylvania State University.
National Climatic Data Center, 2011. NCDC: Global Surface Temperature Anomalies <http://www.ncdc.noaa.gov/cmb-faq/anomalies.php>. National Oceanic and Atmospheric Administration (NOAA).
Olson, R. A., Iraci, L.T., Gore, W.J., Tadic, J., Yates, E.L., 2011, In situ measurements of carbon dioxide and methane over the Sierra mountains of central California and western Nevada, Poster A33C-0234, Presented at the Fall Meeting of the American Geophysical Union, San Francisco, December 7, 2011.
Olsen, S.C. and Randerson, J.T., 2004. Differences Between Surface and Column Atmospheric CO_2 and Implications for Carbon Cycle Research, JGRD 10902301O
Plasynski S., Litynski, J, McIlvried, H., Vikara, D., Srivastava, R., 2011. The critical role of monitoring, verification, and accounting for geologic carbon dioxide storage projects. Environmental Geosciences, V. 18, No. 1, 19-34.
Pillai, D., C. Gerbig, J. Marshall, R. Ahmadov, R. Kretschmer, T.Koch, and U. Karstens, 2010, High resolution modeling of CO_2 over Europe: implications for representation errors of satellite retrievals. Atmos. Chem. Phys., 10, 83–94.
Reichle, D., et al. 1999. Carbon sequestration research and development. DOE/SC/FE-1. U.S. Department of Energy, Washington, DC
Reuter, M., Bovensmann, H., Buchwitz, M., Burrows, J. P., Connor, B., Deutscher, N. M., Griffith, D. W. T., Heymann, J., Keppel-Aleks, G., Messerschmidt, J., Notholt, J., Petri, C., Robinson, J., Schneising, O., Sherlock, V., Velazco, V. A., Warneke, T., Wennberg, P. O., and Wunch, D., 2011. Retrieval of atmospheric CO_2 with enhanced accuracy and precision from Sciamachy: Validation with Fourier transform spectrometer measurements and comparison with model results, J. Geophys. Res., 116, D04301
ing, O., Buchwitz, M., Reuter, M., Heymann, J., Bovensmann, H., Burrows, J.P., 2010. Long-term analysis of carbon dioxide and methane column-averaged mole fractions retrieved from SCIAMACHY, Atmospheric Chemistry and Physics Discussions, Vol. 10, Issue 11, 27479-27522.
Spengler, L.H., Dobeck, L.M., Gullickson, K.S., et al., 2009. A shallow subsurface controlled release facility in Bozeman, Montana, USA for testing near surface CO_2 detection techniques and transport models. Dept. of Chemistry and Biochemistry, Montana State University.
Vigil, S. and Crisp, D., 2010. The Use of Data from the Orbiting Carbon Observatory to Measure Greenhouse Gas Emissions from Landfills. Presented at the 103rd Annual Conference and Exhibition of the Air and Waste Management Association Observatory to Measure Greenhouse Gas Emissions from Landfills, Alberta, Canada, June 22 2010.

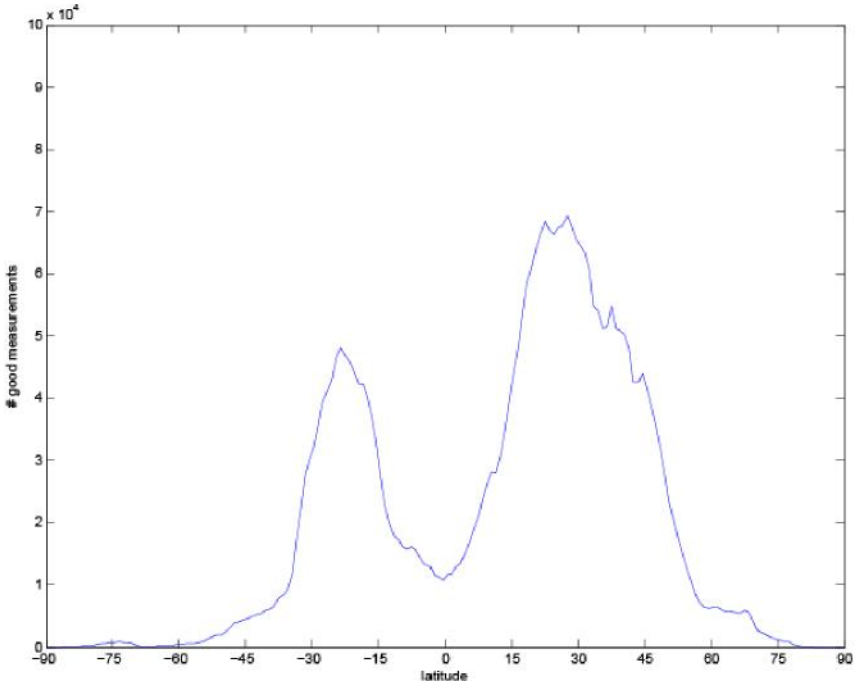

Figure 1: Number of SCIAMACHY CO_2 measurements flagged as "good" for 2003-2005 as a function of latitude.

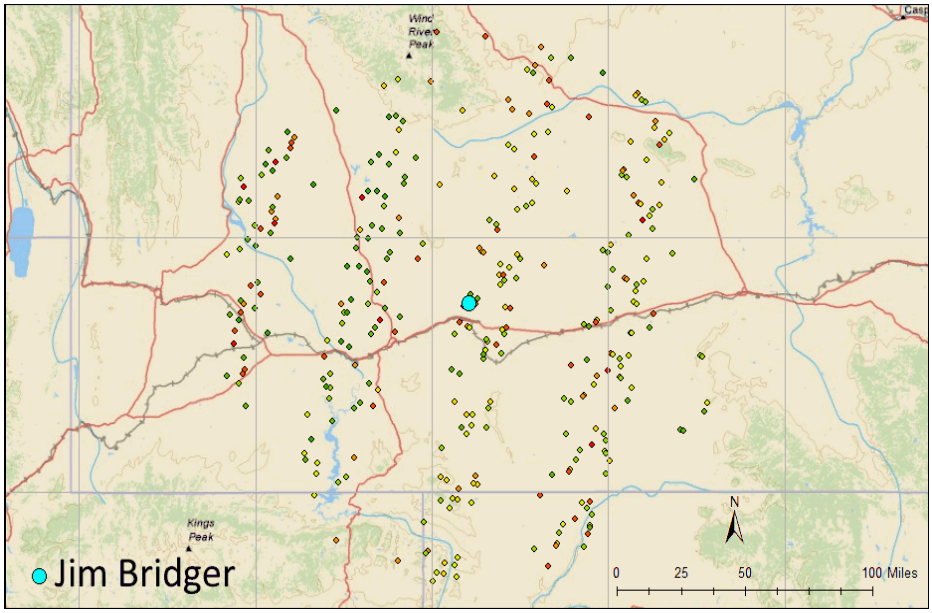

Figure 2: SCIAMACHY data within a 100-mile radius of Jim Bridger power plant from the summer of 2005. Red data points represent high xCO_2 values, green points represent low xCO_2 values.

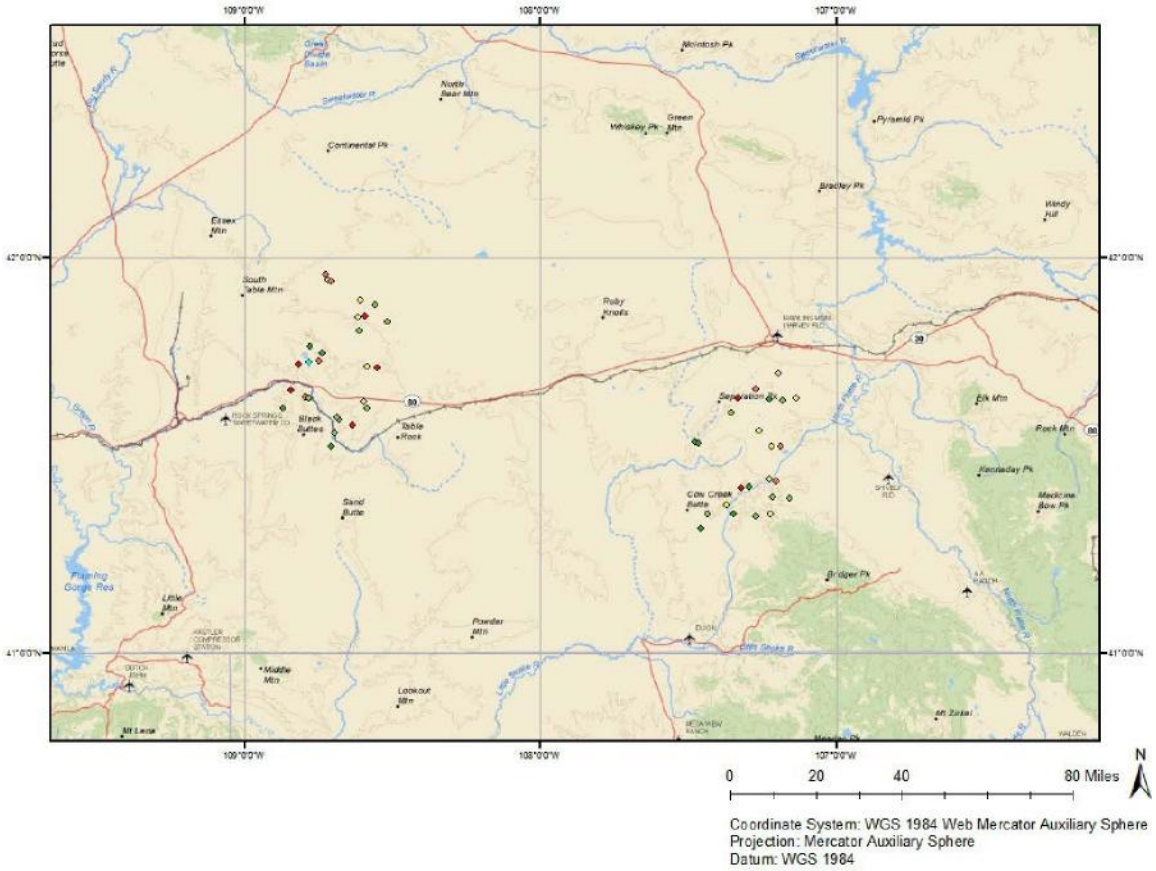

Figure 3: SCIAMACHY data within 20 miles of Jim Bridger and control region 80 miles east. Red data points represent high xCO_2 values, green points represent low xCO_2 values.

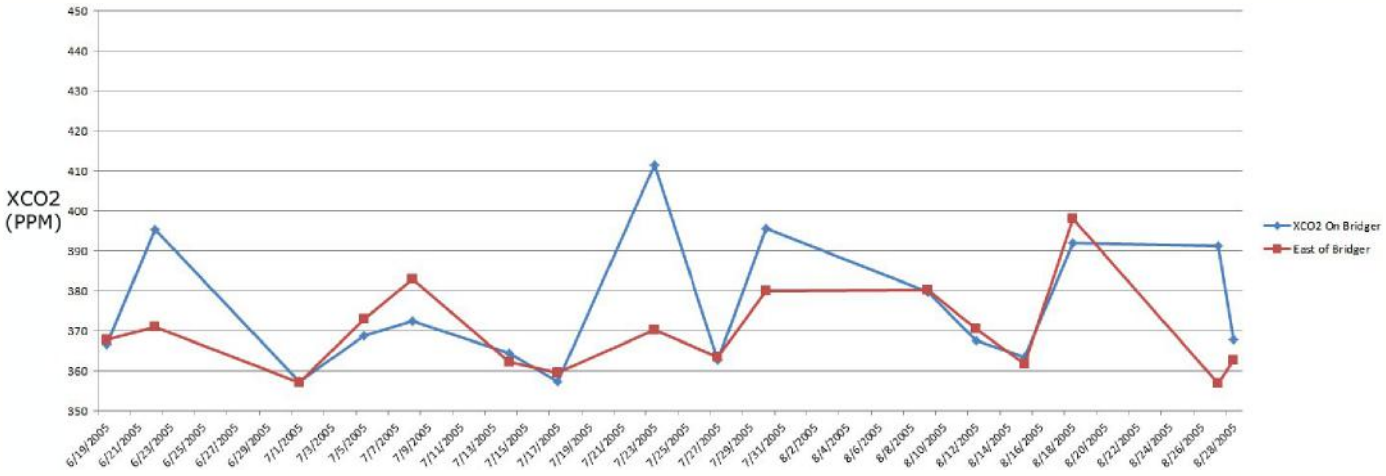

Figure 4: Time-series for Jim Bridger and control region 80 miles east. Lines between points are not interpolations.

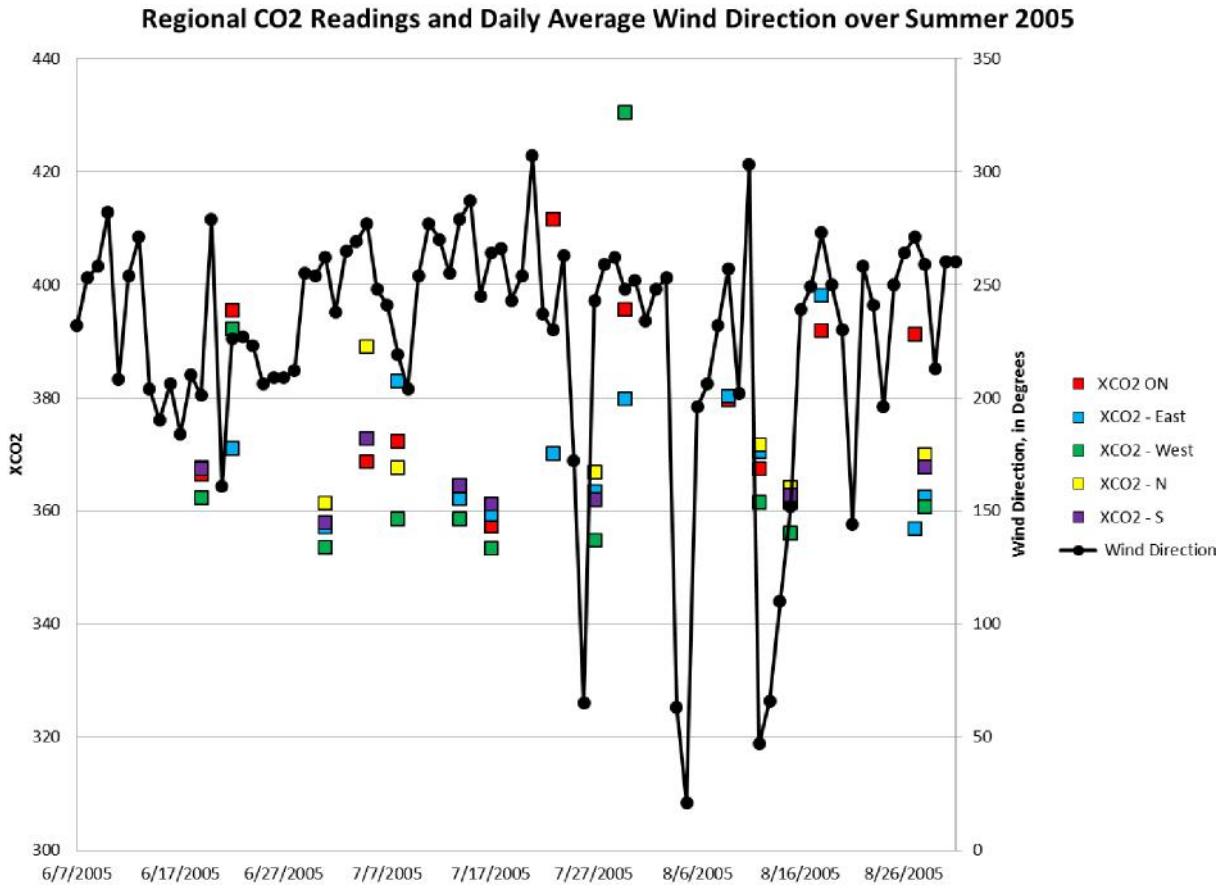

Figure 5: Time-series of xCO_2 near Jim Bridger and 4 adjacent regions, with daily average wind direction.

(a)

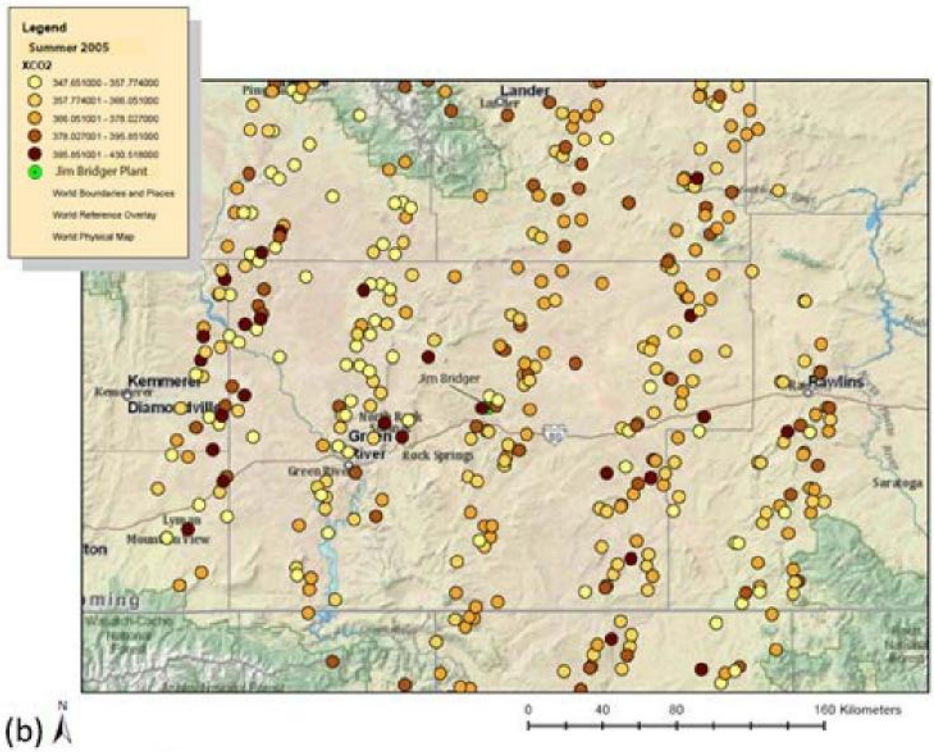

(b)

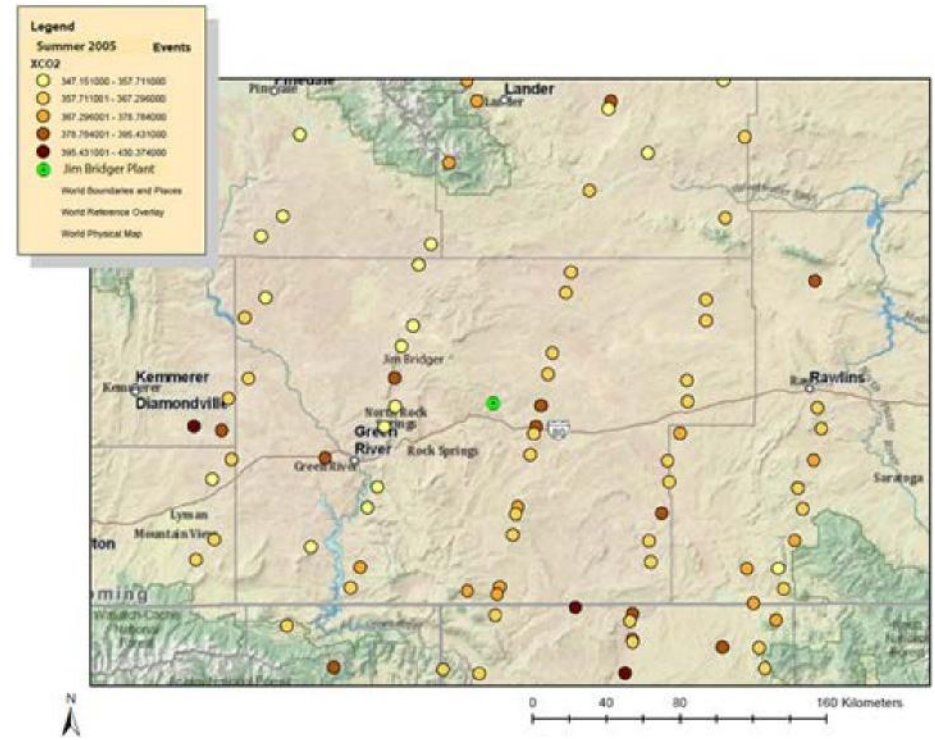

Figure 6: Maps of total xCO_2 readings near Jim Bridger over summer 2005, by general wind orientation. (a) shows points collected on days with average wind directions of 200° to 320° (westerly winds), (b) shows points collected on days with average wind directions of 10° - 170° (easterly winds).

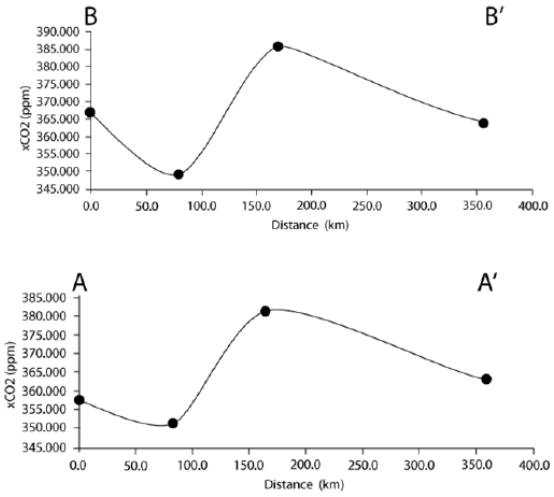

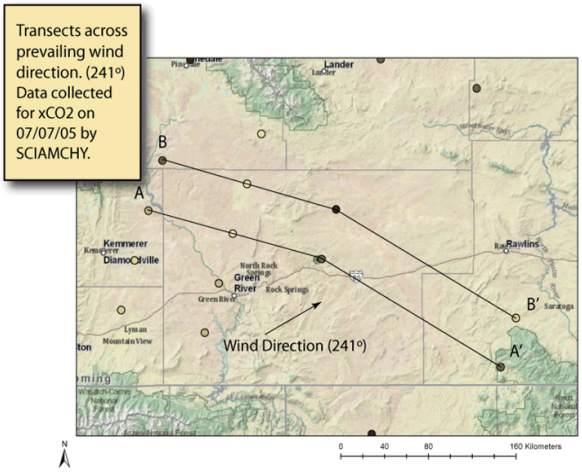

Figure 7: Map of xCO_2 readings near Jim Bridger for days in Summer 2005 in which prevailing wind direction was 241°, with plots along transect A-A' (upper) and transect B-B' (lower). Both are nearly orthogonal to wind direction, 241°. B-B is approximately 40 km NW of A-A'.

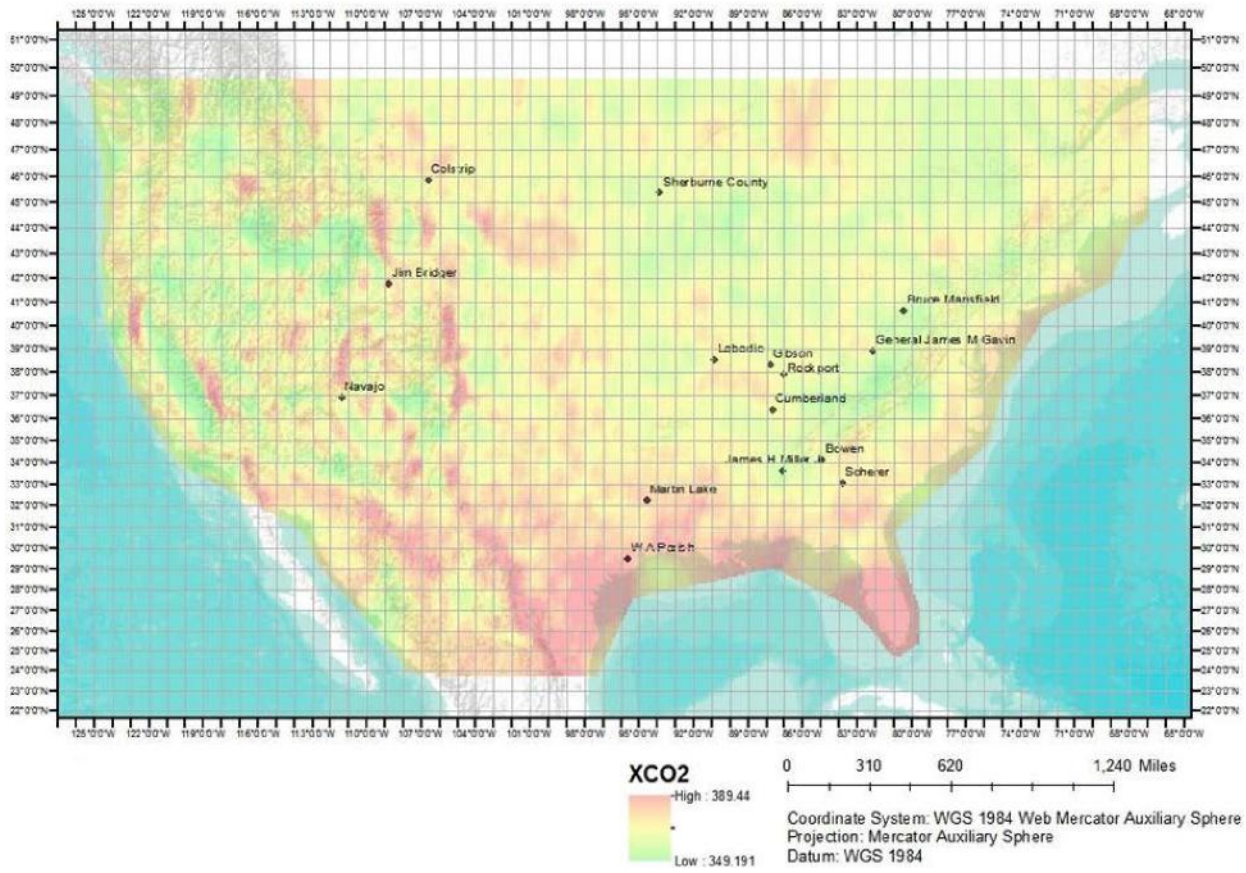

Figure 8: Kriged xCO_2 map of the contiguous US in summer 2005, with high-CO_2-emission electric plants marked.

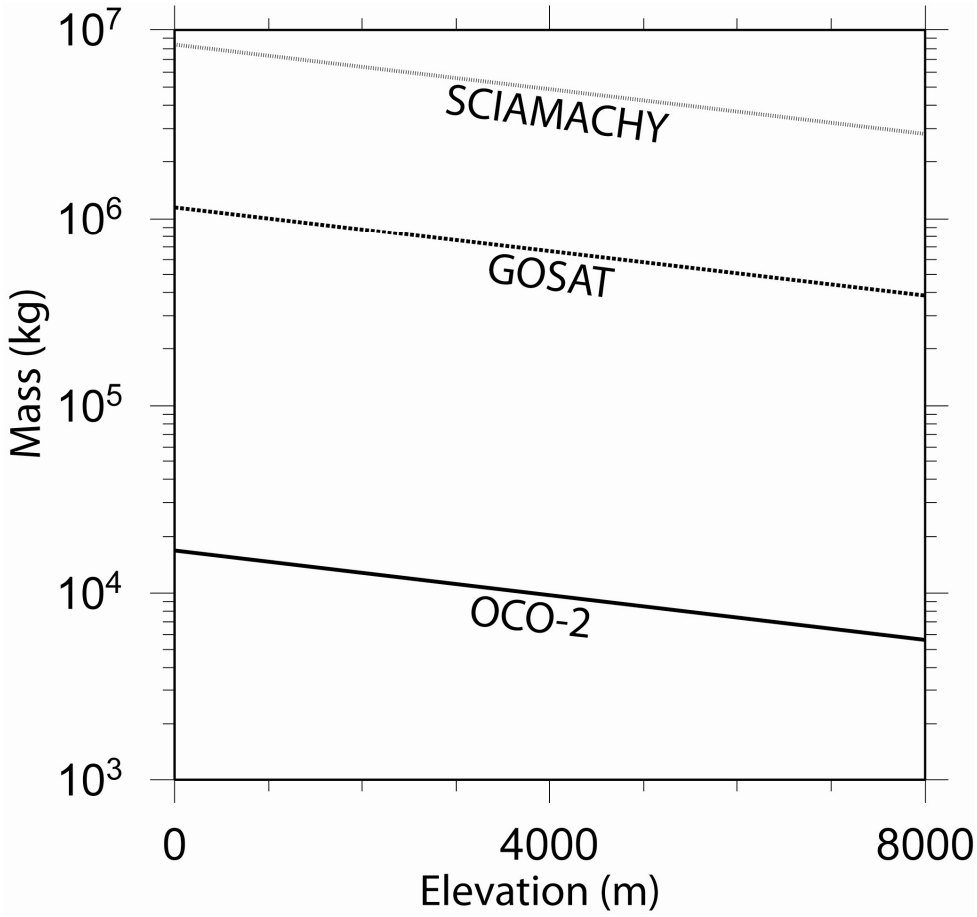

Figure 9: Excess mass needed to raise xCO_2 in the atmosphere of a footprint of GOSAT, SCIAMACHY, and OCO-2 by 1 ppm, as a function of elevation.

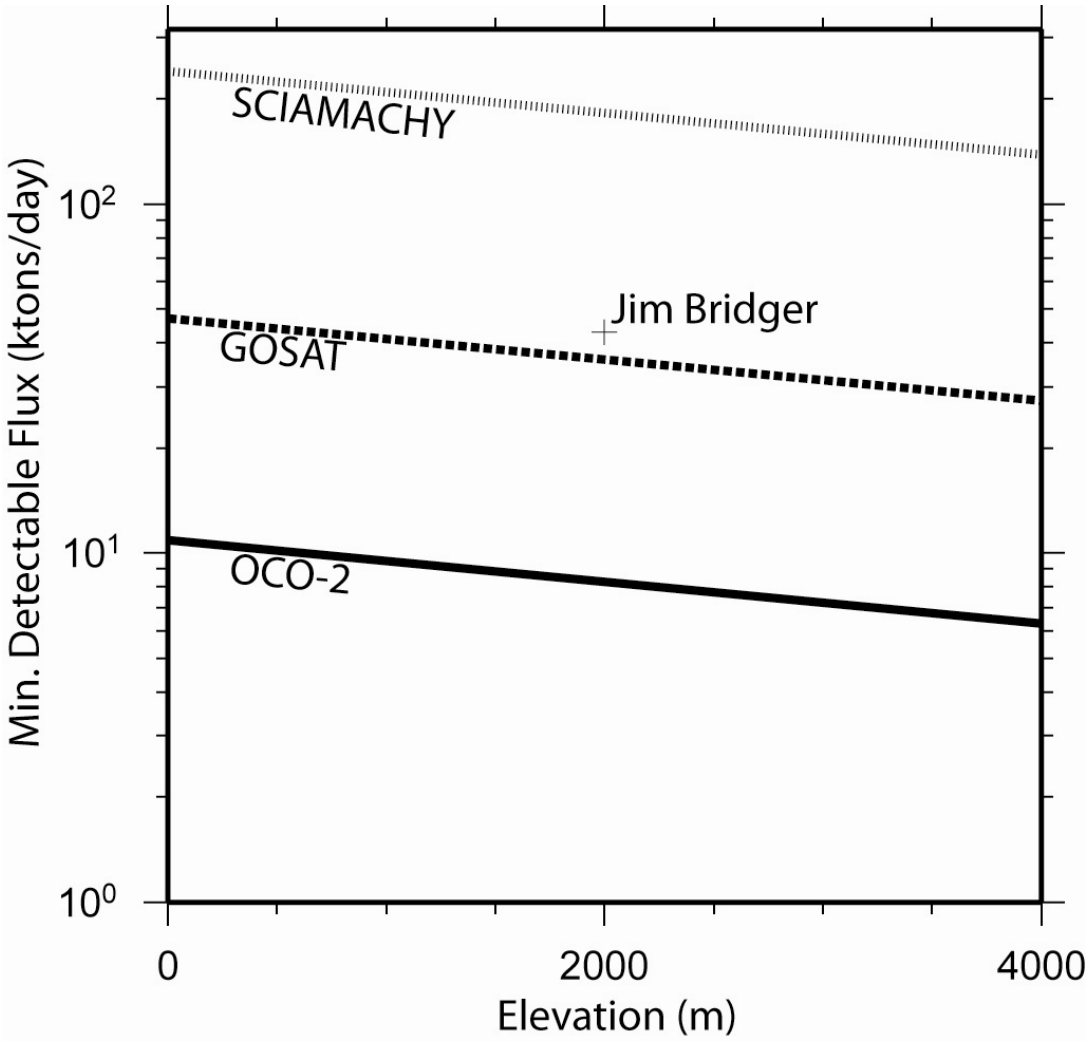

Figure 10: Estimated minimum detectable source flux for OCO-2 as function of elevation for OCO-2, GOSAT, and SCIAMACHY. These values will increase linearly with wind speed.

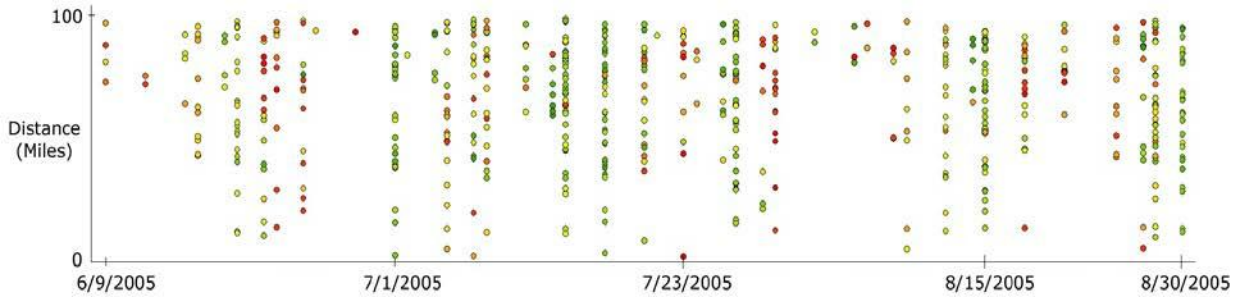

Figure 11: Time series of xCO_2 v. distance from Jim Bridger. xCO_2 is expressed as a color ramp from green (low) to high (red).

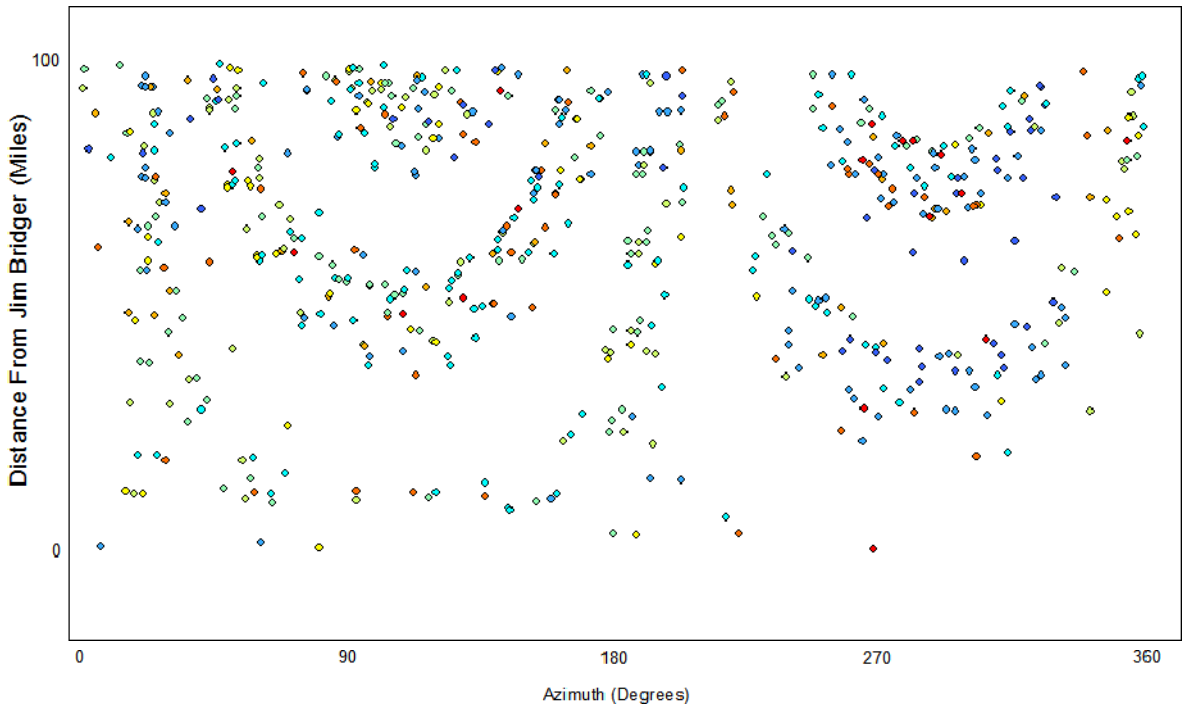

Figure 12: Time series of xCO_2 v. distance and azimuth from Jim Bridger. xCO_2 is expressed as a color ramp from blue (low) to high (red)

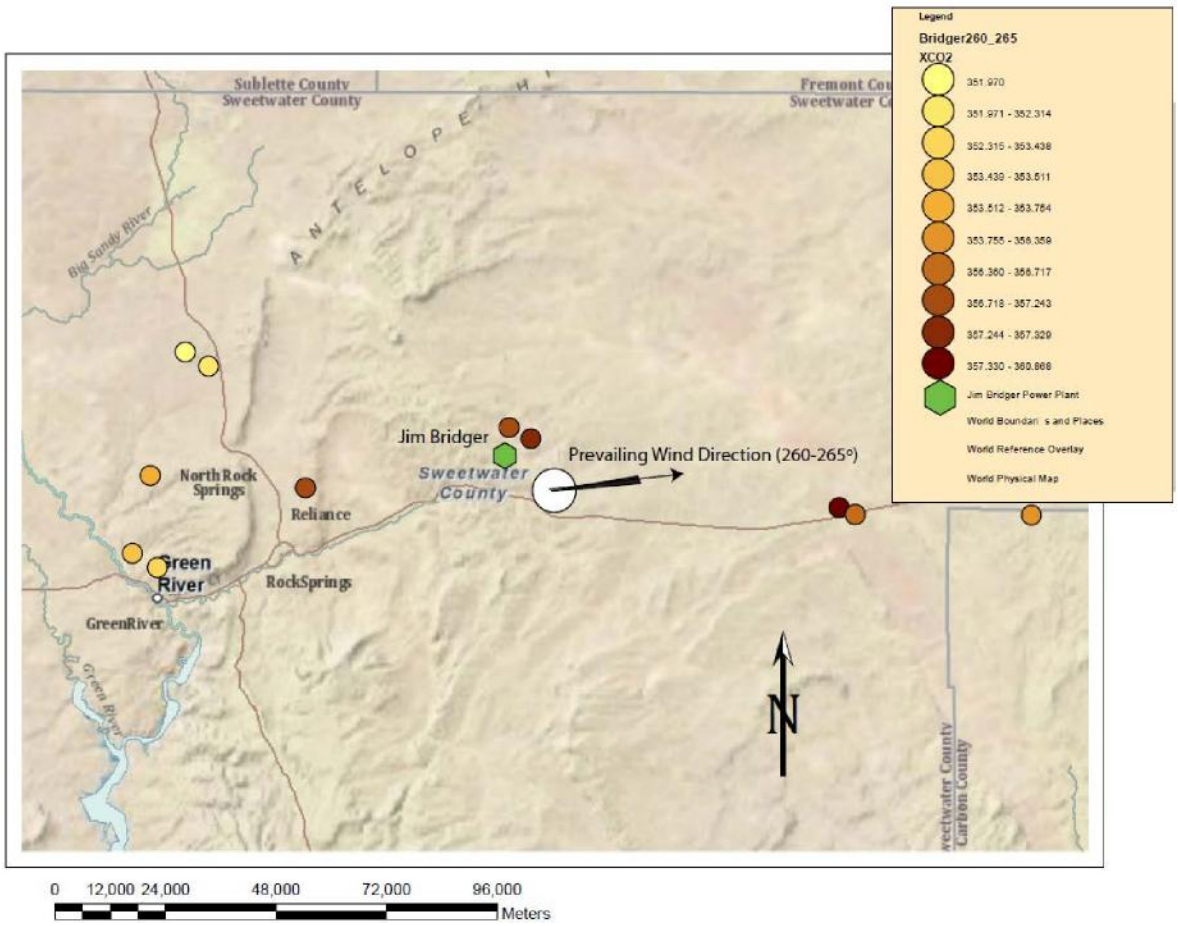

Figure 13: Map of xCO_2 readings binned by wind direction (260˚-265˚) over summer 2005.

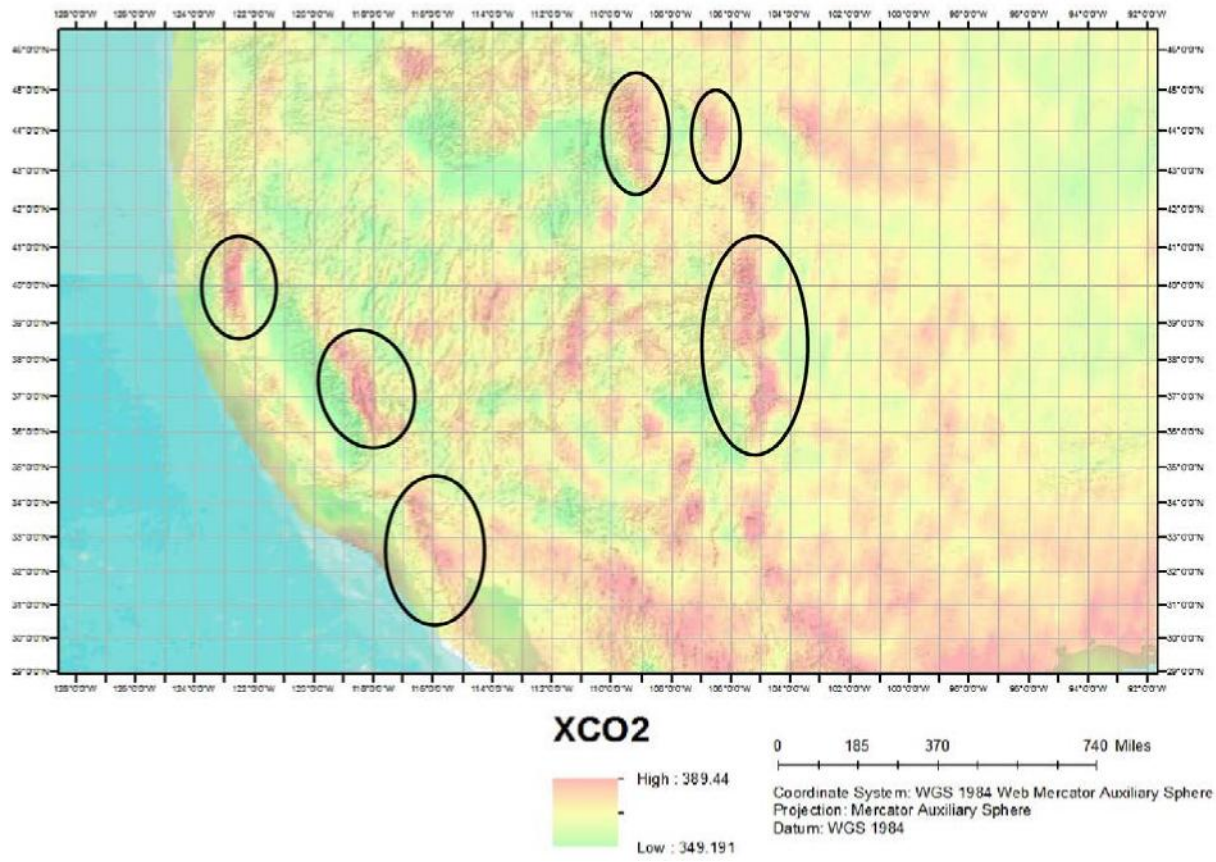

Figure 14: Kriged map of the western US, with some examples of the range-side high pattern circled.

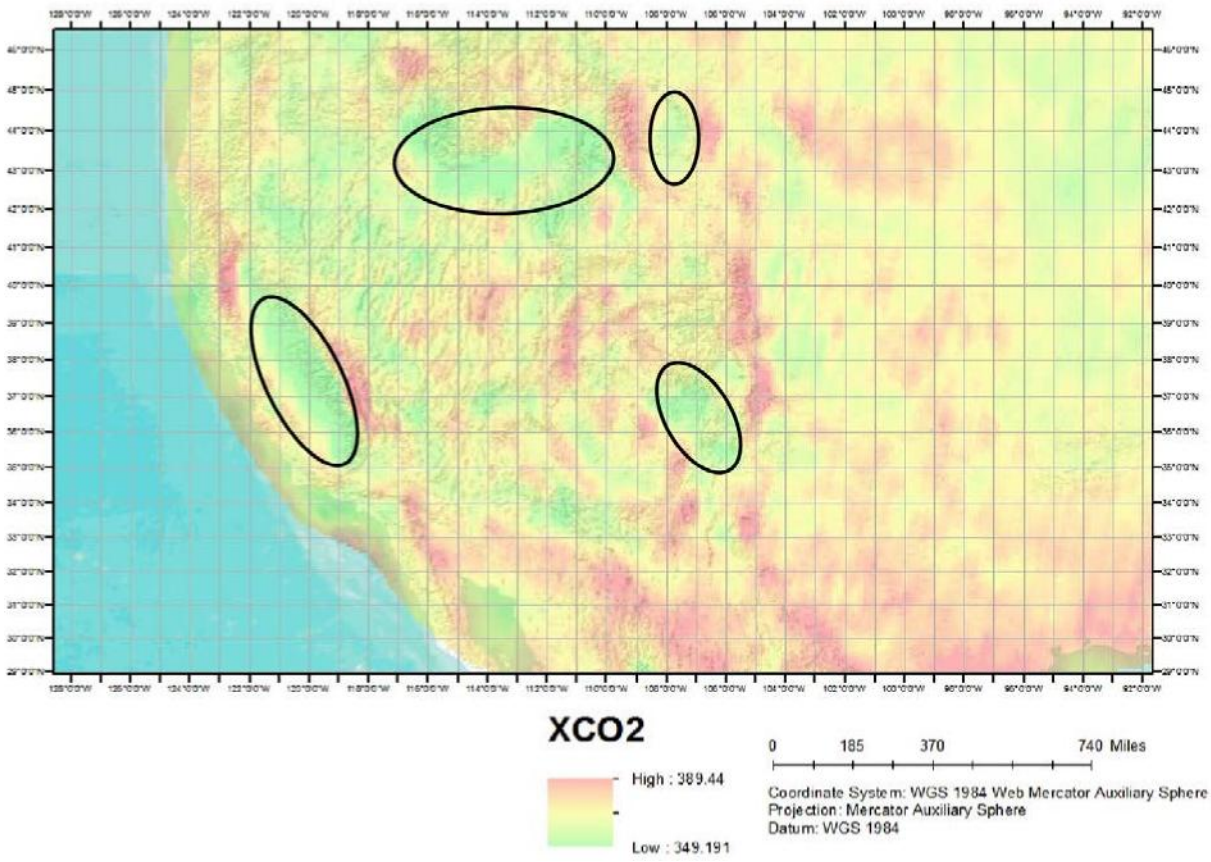

Figure 15: Kriged map of the western US, with some examples of the basin low pattern circled.

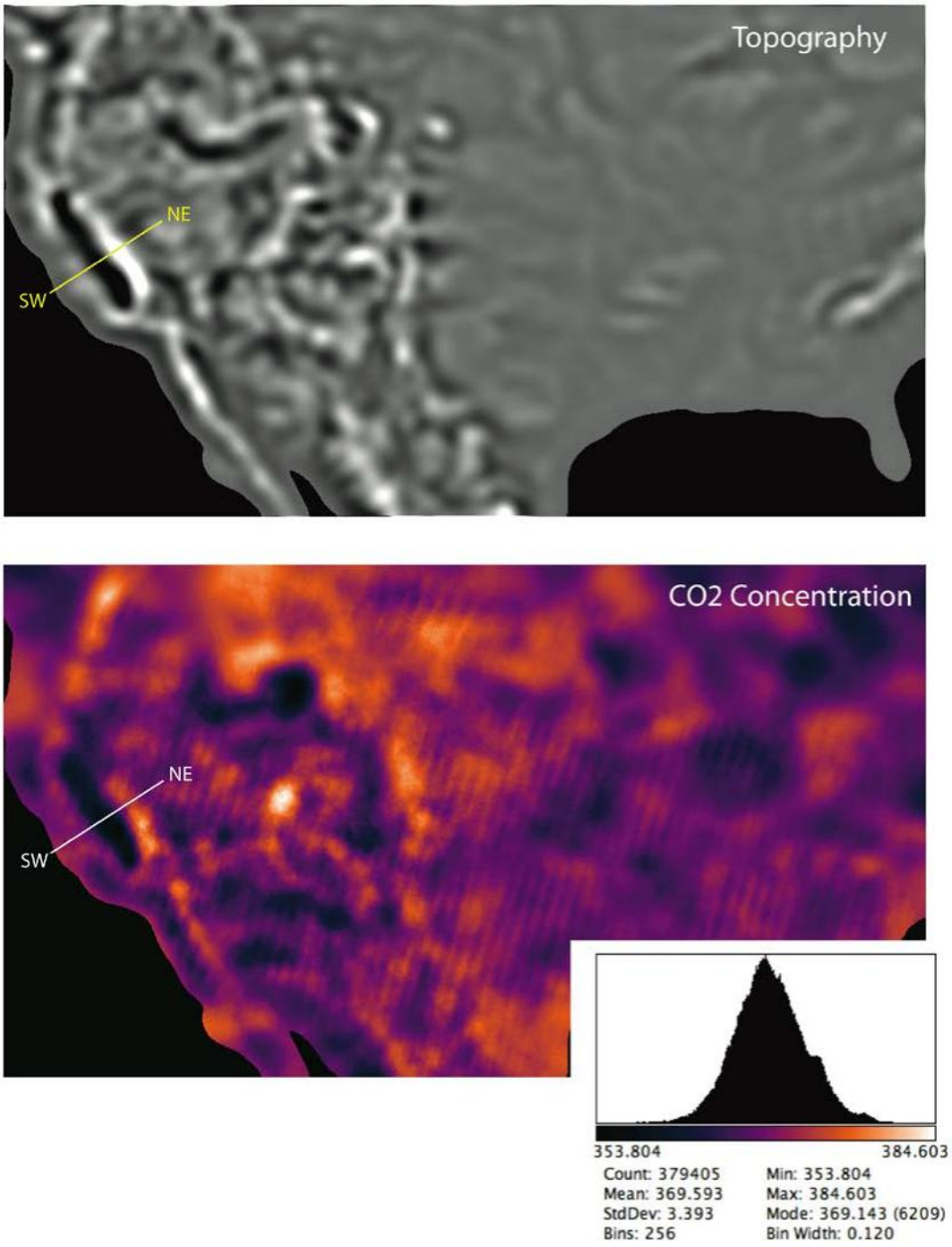

Figure 16: Correlation of topography (upper grey-scale image) with CO_2 concentration from Kriged SCIAMACHY data over the US. The SW-NE line shows the transect used to compare topography and CO_2 (see Figure 17).

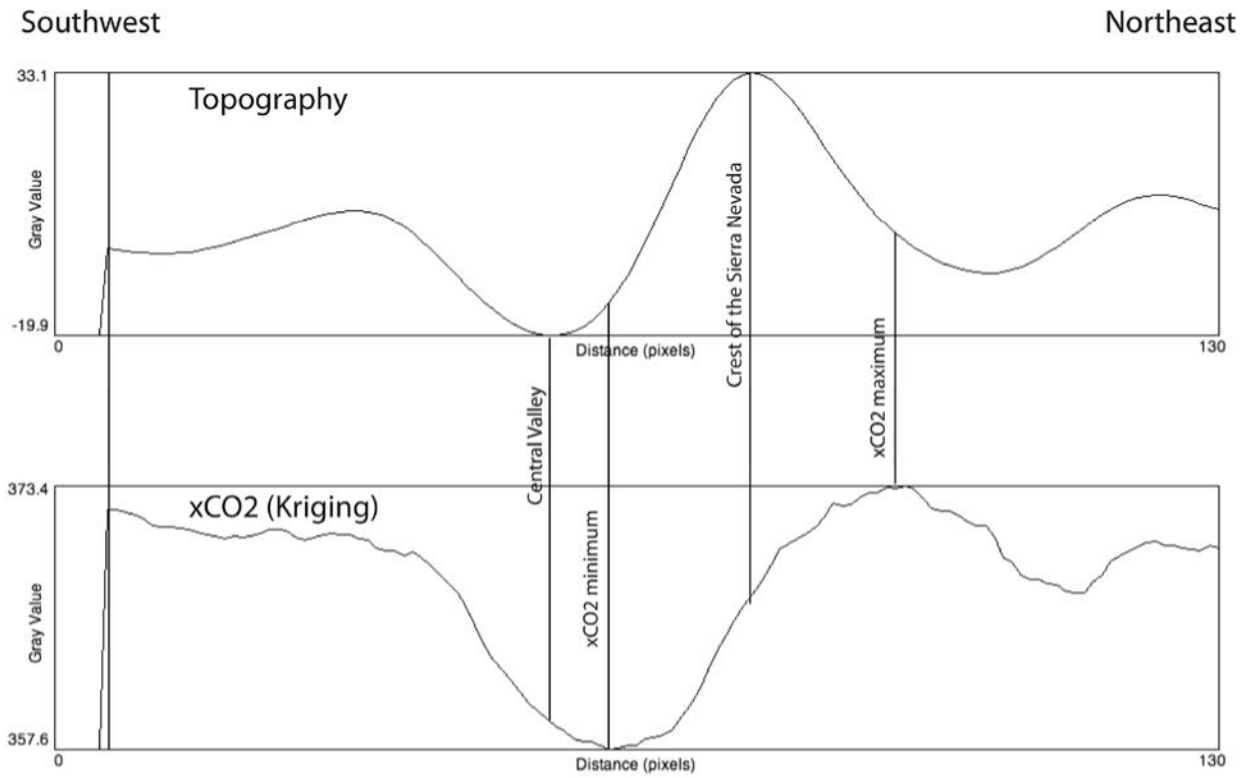

Figure 17: Comparison of CO_2 concentrations and topography along a SW-NE transect across California's Central Valley and Sierra Nevada.